Electronic Structure of BCl Determined by Ab Initio Calculations and Resonance-Enhanced Multiphoton Ionization Spectroscopy†

Karl K. Irikura,* Russell D. Johnson, III,* and Jeffrey W. Hudgens*

Physical and Chemical Properties Division, Chemical Science and Technology Laboratory, National Institute of Standards and Technology, Gaithersburg, Maryland 20899

Received: November 10, 1999; In Final Form: January 20, 2000

The mass-resolved, one-color, 2 + 1 resonance-enhanced multiphoton ionization spectrum of transient boron monochloride (BCl) between 348 and 369 nm is reported. Vibrational and rotational bands of the $^{10}B^{35}Cl$, $^{11}B^{35}Cl$, $^{10}B^{37}Cl$, and $^{11}B^{37}Cl$ isotopomers and two previously unreported electronic states are assigned. Rotational analysis identifies the F $^1\Sigma^+$ (3sσ) state ($\nu_{00} = 55994 \pm 10$ cm^{-1} for $^{11}B^{35}Cl$). EE-EOM-CCSD ab initio calculations for BF and BCl support the F state assignment and suggest a tentative assignment of b $^3\Sigma^+$ (3pσ) ($\nu_{00} = 56864 \pm 10$ cm^{-1} for $^{11}B^{35}Cl$). Uncertainties indicate the confidence of two standard deviations.

Introduction

The transient molecule BCl is of interest due to its importance in radio frequency (rf) plasmas that use BCl_3 feed-gas to etch metals and semiconductor materials.[1−4] In these rf plasmas, BCl_3 is believed to produce BCl through a two-step sequence involving Penning ionization of BCl_3 through collisions with metastable argon and dissociative recombination of BCl_3^+ with an electron.[5−7] To account for chemical and electrical properties of the plasma, computational models need to include the electronic structure, the ionization energy, and the electron affinities of all BCl_n ($n = 0-3$) neutral and ionic products.

Collected spectroscopic and thermochemical data of BCl have a history of dispute, and inconsistencies persist in the literature regarding the ionization energy and the assignments of electronic states. Mass spectrometric measurements, mostly based on electron impact ionization, have yielded values for the adiabatic ionization energy of BCl that range between 12 and 9.9 eV.[8−11] In contrast, the recent spectroscopic determination found a value of $IE_a(BCl) = 9.03$ eV by extrapolation of $^1\Sigma^+$ (3sσ) and $^1\Sigma^+$ (4sσ) members of a Rydberg series.[12] Although such extrapolations have a history of determining IE_a's with an uncertainty approaching ±0.001 eV, this particular spectroscopic determination is about 1 eV lower than found by the most recent experiments[9] and by ab initio calculations.[13,14] This inconsistency suggests that the Rydberg character of these $^1\Sigma^+$ states is misassigned and, consequently, that a previously unobserved $^1\Sigma^+$ band system originating from the true 3sσ Rydberg state resides at lower energy. The observation of this band system would bring the spectroscopic and mass spectrometric data into accord.

This study reports experiments and ab initio calculations that expand upon the spectroscopic data for BCl. We report the discovery of two new electronic states of BCl and describe their vibrational and rotational analyses. We also report extensive ab initio calculations of the electronic spectra of BF and BCl. These calculations guide reassignments of recently reported electronic states and reconcile the determinations of $IE_a(BCl)$ by optical spectroscopy and mass spectrometry.

† Part of the special issue "Marilyn Jacox Festschrift".

* Corresponding authors. E-mail addresses: karl.irikura@nist.gov; russell.johnson@nist.gov; jeffrey.hudgens@nist.gov.

Experimental Procedure

The apparatus is described in detail elsewhere.[15] Briefly, the experimental apparatus consisted of a sampled flow reactor, a pulsed tunable dye laser, a time-of-flight (TOF) mass spectrometer, and a computer-controlled data acquisition system. In the flow reactor, BCl was generated by reacting a stoichiometric excess of atomic chlorine, produced by passing 10% Cl_2 in helium through a microwave discharge (2450 MHz, 30 W), with 10% B_2H_6/90% He. The flow velocity of the reactor was typically 1−3 m/s, and the total pressure was 200 Pa (1.5 Torr). This mixture was allowed to react and was then effusively sampled by a large-orifice (∼1 mm) skimmer, while the majority of the gas mixture was pumped away. The effusive flow entered the ion extraction region of the TOF mass spectrometer, where it intersected with the focused beam (focal length = 250 mm) of a pulsed excimer-pumped dye laser (energy = 10 mJ/pulse; bandwidth = 0.8 cm^{-1}, fwhm; 20 ns duration). The ions were accelerated, focused, mass separated, and detected by a Daly ion detector.[16] Four separate gated integrator/boxcar averagers were used to monitor simultaneously the signals from the four isotopic products $^{10}B^{35}Cl^+$, $^{10}B^{37}Cl^+$, $^{11}B^{35}Cl^+$, and $^{11}B^{37}Cl^+$. A computerized data acquisition system collected and averaged the mass-resolved signals. The TOF mass spectrum was displayed on the oscilloscope to ascertain the product masses and to ensure that unit mass resolution was achieved. As is customary, the spectra presented here do not incorporate corrections for laser power variation across the laser dye efficiency profiles; however, the data that comprise these figures were selected to minimize any abrupt signal intensity changes due to laser performance.

Results

Experimental Spectra. Figure 1 shows the *m*/*z* 46 resonance-enhanced multiphoton ionization (REMPI) spectrum of $^{11}B^{35}Cl$ observed between 348 and 369 nm. Similar REMPI spectra were carried by *m*/*z* 45 ($^{10}B^{35}Cl^+$), *m*/*z* 47 ($^{10}B^{37}Cl^+$), and *m*/*z* 48 ($^{11}B^{37}Cl^+$), indicating that these spectra originate from BCl. Table 1 lists the wavelengths of the peaks in each isotopically selected spectrum as well as the assignment, two-photon energy of the transition, the energy relative to the electronic origin, and the isotopic shift relative to the $^{11}B^{35}Cl$ spectrum.

10.1021/jp994011u
Published on Web 03/14/2000

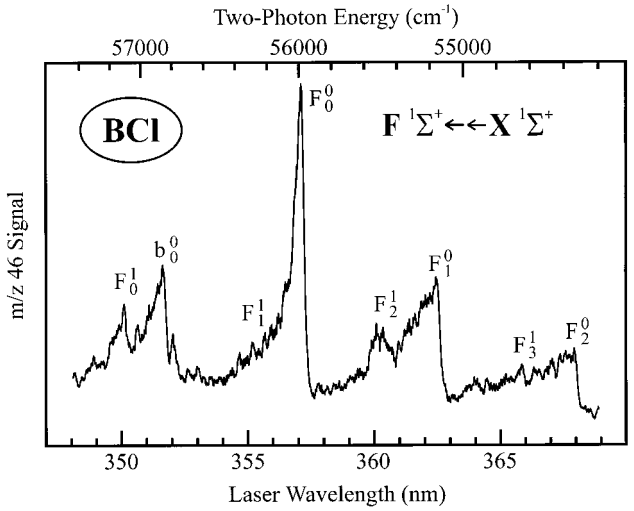

Figure 1. 2 + 1 REMPI spectrum of $^{11}B^{35}Cl$ (m/z 46) between 348 and 369 nm.

Vibrational analyses, rotational analyses, and ab initio results indicate that the REMPI spectrum arises through two-photon absorption by the upper electronic state. The prominent bands near 357.1 and 351.6 nm exhibit appropriate isotope shifts indicating assignments as electronic origins. The isotope shifts are calculated using eqs 1−5,[17] where μ is the reduced mass of $^{11}B^{35}Cl$ (8.373167 u) and μ^i is the reduced mass of the other isotope: $^{10}B^{35}Cl$ (7.784059 u), $^{10}B^{37}Cl$ (7.878808 u), or $^{11}B^{37}Cl$ (8.482900 u).

$$\rho = \sqrt{\mu/\mu^i} \tag{1}$$

$$\omega^i = \rho\omega \tag{2}$$

The vibrational levels for different isotopes are given by eqs 3−5, where E is the energy of the observed transition, and T_e is the energy difference between the minima of the upper- and ground-state Born−Oppenheimer potential energy curves. Thus, a given transition $E(v'v'')$ will be shifted by the amount in eq 5. Using $\omega'' = 828$ cm^{-1} and $\omega' = 1119$ cm^{-1} (appropriate for $^{11}B^{35}Cl$; see below) yields the predicted isotope shifts shown in Table 1.

$$G(v) = \omega(v + 1/2) \tag{3}$$

$$E = T_e + G(v') - G(v'') \tag{4}$$

$$E^i - E = (\rho - 1)[\omega'(v' + 1/2) - \omega''(v'' + 1/2)] \tag{5}$$

We designate the bands shown in Figure 1 as F_0^0 and b_0^0, respectively, where the symbol $S_{v''}^{v'}$ indicates the number of vibrational quanta in the upper and ground electronic states. The F_0^0 origin assignments are supported by the hot band structure. Previous UV absorption studies of $^{11}B^{35}Cl$ have established that the $v'' = 1$ and $v'' = 2$ levels of the ground-state manifold lie at 829 and 1648 cm^{-1} above $v'' = 0$, respectively.[18,19] The $^{11}B^{35}Cl$ spectrum displays these hot bands at 362.44 and 367.88 nm, respectively. The spectrum of each BCl isotopomer also displays F_1^0 and F_2^0 hot bands at energy intervals that are in accord with the previous infrared determinations.[18] To the blue of each F_0^0 band, each isotopomer spectrum exhibits one vibrational level of the F state near 350 nm, which determines the vibrational intervals in the F states, $\Delta G'_{1/2} = G'(1) - G'(0)$. These determinations of $\Delta G'_{1/2}$ are supported by a consistent set of sequence band assignments (Table 1), which also conform to the predictions of the reduced mass relationships for vibrational levels (eqs 1−5).

TABLE 1: REMPI Bands Displayed in the Mass Selected Spectra

assign. $S_{v''}^{v'}$	λ_{laser} (nm)	two-photon energy[a] (cm^{-1})	$\nu^i - \nu_{00}$ (cm^{-1})	isotopic shift[b] (cm^{-1})	predicted shift[c] (cm^{-1})
		$^{10}B^{35}Cl$			
F_0^1	349.82	57 156	1157	43	45
b_0^0	351.58	56 870	871	6	5
F_0^0	357.05	55 999	0	5	5
$\{F_2^1\}^d$	360.77	55 422	−577	−87	−14
F_1^0	362.60	55 141	−858	−25	−24
F_3^1	365.93	54 639	−1360	−22	−44
F_2^0	368.26	54 295	−1704	−55	−54
		$^{11}B^{35}Cl$			
F_0^1	350.08	57 113	1119		
b_0^0	351.62	56 864	870		
F_1^1	355.24	56 284	290		
F_0^0	357.08	55 994	0		
F_2^1	360.20	55 509	−485		
F_1^0	362.44	55 166	−828		
F_3^1	365.79	54 661	−1333		
F_2^0	367.88	54 350	−1644		
		$^{10}B^{37}Cl$			
F_0^1	349.78	57 162	1167	49	38
b_0^0	351.63	56 862	867	−2	4
F_0^0	357.07	55 995	0	1	4
F_2^1	360.41	55 477	−518	−32	−12
F_1^0	362.49	55 158	−837	−8	−20
$\{F_3^1\}^d$	366.25	54 592	−1403	−69	−37
$\{F_2^0\}^d$	367.85	54 355	−1640	5	−45
		$^{11}B^{37}Cl$			
F_0^1	350.00	57 126	1134	13	−8
b_0^0	351.63	56 863	871	−1	−1
F_0^0	357.09	55 992	0	−2	−1
F_2^1	360.19	55 511	−481	2	3
F_1^0	362.42	55 169	−823	3	4
F_3^1	365.80	54 660	−1332	−1	8
F_2^0	367.85	54 354	−1638	4	10

[a] Relative uncertainty (2σ) of each interval between two intensity maxima is ±3 cm^{-1}, and the absolute uncertainty (2σ) of each maximum is ±10 cm^{-1}. [b] The frequency shift of each transition relative to the corresponding transition in $^{11}B^{35}Cl$, i.e., ν^i(species) − ν^i($^{11}B^{35}Cl$). [c] Using the mass ratios given in the text and $\omega'' = 1119$ and $\omega' = 828$ cm^{-1}. [d] Tentative assignment.

The expected hot band structure of the b−X REMPI band system is overlapped by the more intense F←←X system, obscuring these bands from identification. Lacking the hot band data, a direct proof of the photon order of the resonant state is not possible. In the Discussion, we use the results of ab initio calculations to establish that the b state resides at the sum of two laser photons ($\nu_{00} \approx 57\,000$ cm^{-1}) and that the band at $\lambda_{laser} \approx 351.6$ nm is the electronic origin.

Each isotopic F_0^0 origin band displays a single strong branch (Figure 2), which suggests a $^1\Sigma-^1\Sigma$ or $^1\Delta-^1\Sigma$ two-photon transition. The calculations do not predict a Δ state in this energy region, so the transition is assigned as $^1\Sigma-^1\Sigma$. Weak O and S branches are also observed, consistent with a $^1\Sigma-^1\Sigma$ transition. Least-squares fitting of a quadratic expression ($aJ^2 + bJ + c$) to the rotational lines yields ΔB ($= a$), the difference between the rotational constants of the excited and ground states. When the J levels are correctly indexed, the least-squares fit satisfies $a = b$ and also yields the position c of the rotationless origin.

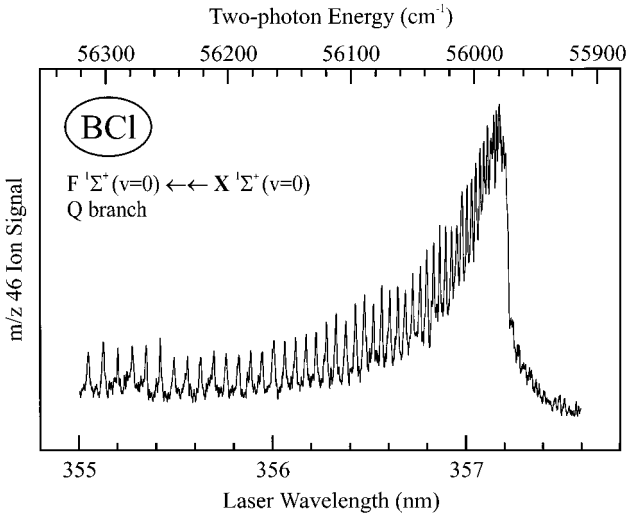

Figure 2. 2 + 1 REMPI spectrum showing the rotational structure of the F $^1\Sigma^+(v'' = 0) \leftarrow\leftarrow$ X $^1\Sigma^+(v' = 0)$ transition of $^{11}B^{35}Cl$ (m/z 46).

The Q branch is almost completely resolved into distinct rotational lines. However, the O and S branches are much weaker and overlapped by the Q branch lines, making them less useful for determining rotational constants. The fit of the Q branch data from the $^{11}B^{35}Cl$ spectrum yields $\Delta B_o = (0.1112 \pm 0.0005)$ cm^{-1}. Using the ground-state spectroscopic constants for $^{11}B^{35}Cl$,[19] we derive the rotational constant of the F $^1\Sigma^+$ state, $B_0' = 0.782 \pm 0.002$ cm^{-1} in $^{11}B^{35}Cl$, which corresponds to an internuclear distance $r_0 = 1.605 \pm 0.006$ Å. For comparison, the ground state of $^{11}B^{35}Cl$ has a longer internuclear distance, $r_0 = 1.7327 \pm 0.0002$ Å. The shorter bond in the upper state is consistent with the ~300 cm^{-1} increase in the vibrational frequency interval, $\Delta G_{1/2}$, observed between the X $^1\Sigma^+$ and the F $^1\Sigma^+$ state. Thus, these properties indicate that the F $^1\Sigma^+$ state is more tightly bound than the ground state.

Table 2 summarizes the spectroscopic constants derived from the spectrum of each BCl isotopomer. We note that the rotational constants, B_0', obtained from the analyses of the Q branches of $^{10}B^{35}Cl$, $^{11}B^{35}Cl$, and $^{11}B^{37}Cl$ yield identical internuclear distances, $r_0 \approx 1.605$ Å.

Ab Initio Calculations. Ab initio calculations were performed to aid in the assignment of the experimental spectra and to provide predictions for unobserved electronic states. Calculations were first performed for the BF molecule, which is isovalent with BCl, to assess the reliability of the comparisons. Potential energy curves were calculated at the well-correlated EE-EOM-CCSD level[20] using the reasonably large aug-cc-pVTZ basis sets[21,22] augmented with additional diffuse functions to accommodate Rydberg states. One s, one p, and one d shell were added on each atomic center. The exponents were $\alpha_s(B) = 0.0099$, $\alpha_s(F) = 0.027$, $\alpha_s(Cl) = 0.021$, $\alpha_p(B) = 0.0057$, $\alpha_p(F) = 0.020$, $\alpha_p(Cl) = 0.013$, $\alpha_d(B) = 0.018$, $\alpha_d(F) = 0.100$, and $\alpha_d(Cl) = 0.053$. A tight d function, $\alpha_d(Cl) = 3.181$, was added to chlorine to compensate for known deficiencies.[23−25] This yields 110 contracted functions on BF and 119 functions on BCl. A spin-restricted (RHF) reference was used for singlet states and a spin-unrestricted (singlet UHF) reference was used for triplet states. Potential energy curves for the molecular ions were computed at the CCSD level for direct comparison with the neutral calculations. Equilibrium geometries (r_e) and excitation energies (T_e) were determined by parabolic interpolation between computed points on the potential energy curves, which were spaced 0.05 or 0.10 Å apart. Vibrational levels were computed assuming the most abundant isotopes (i.e., reduced masses of 6.970183 u for ^{11}BF and 8.373167 u for $^{11}B^{35}Cl$) and using the Fourier-grid Hamiltonian method.[26] Vibrational constants were derived by fitting the lowest few (three to six) vibrational levels to the expression $G(v) = \omega_e(v + {}^1/_2) - \omega_e x_e(v + {}^1/_2)^2$. Where only two quasi-bound levels were found, only $G_{1/2} = G(1) - G(0)$ was computed. For the higher Rydberg states, adiabatic excitation energies T_e relative to the ground state were estimated assuming that $r_e' = r_e(BX^+)$, that is, $T_e \approx E'(r = r_{e,ion}) - E''(r = r_e')$. To accommodate the diffuse electron distributions in these states, additional diffuse basis functions were added in an even-tempered manner, up to a total of three s, three p, and two d shells beyond the basic aug-cc-pVTZ basis sets. The results, included in Tables 3 and 4, are expected to be upper bounds on the correct values of T_e. Adiabatic ionization energies were computed at the CCSD(T) level[27] and extrapolated to the limit of a complete basis set. As recently recommended for computing the atomization energies of BF and BF_3,[28] we accept the largest-basis value for the Hartree−Fock contribution to IE_a and adopt the $A + Bn^{-3}$ extrapolation procedure for the CCSD and (T) correlation contributions.[29] For this purpose, the aug-cc-pVnZ basis sets for chlorine were augmented with a set of tight d functions. The corresponding exponent for $n = 3$ was as indicated above, and $\alpha_d = 3.831$ and 9.35 for $n = 4$ and 5, respectively. Computed bond lengths were 1.265 Å for BF, 1.211 Å for BF^+, 1.713 Å for BCl, and 1.594 Å for BCl^+, which are in good agreement with the previous calculations summarized in ref 14. IE_a was computed from the equilibrium value by applying the zero-point vibrational energies indicated by the computed spectroscopic constants in Tables 3 and 4. Details of the basis set extrapolation, which yielded $IE_a(BF) = 11.10 \pm 0.02$ eV and $IE_a(BCl) = 9.96 \pm 0.04$ eV, are given in Table 5. These calculations may be described concisely as CCSD(T)/CBS(aug-cc;4,5)//CCSD/aug-cc-pVTZ+spd. The uncertainties indicated are the difference between the $n = 3-4$ and $n = 4-5$ extrapolations and are expected to represent a confidence interval of about 90%. Analogous atomic calculations (including spin−orbit corrections) yield IE(B) = 8.30 eV and electron affinities EA(F) = 3.42 eV and EA(Cl) = 3.64 eV, which are in satisfactory agreement with experimental values IE(B) = 8.29803 ± 0.00002 eV, EA(F) = 3.401190 ± 0.000004 eV, and EA(Cl) = 3.6135 ± 0.0010 eV.[30,31] Our molecular ionization energies are in good agreement with earlier high-level calculations, which gave $IE_a(BF) = 11.07$ eV,[14] $IE_a(BCl) = 9.94$ eV,[14] and $IE_a(BCl) = 9.93$ eV.[13] All open-shell calculations were spin-unrestricted. All electrons were correlated in all calculations. The ACES II program package was used for all the ab initio calculations.[32−34]

Ab initio results for BF and BF^+ are collected in Table 3 for comparison with experimental data. The largest systematic discrepancy is for ω_e, for which the computed values are too high by about 25 cm^{-1} for the valence states and by about 50 cm^{-1} for the Rydberg states. The computed equilibrium bond lengths r_e are generally within 0.003 Å of the experimental values. Excitation energies T_e are mostly within 700 cm^{-1} of experimental values. Vibrational anharmonicity constants $\omega_e x_e$ are all within 1.2 cm^{-1} of available experimental values. The computed adiabatic ionization energy is 11.10 ± 0.02 eV, which agrees well with the experimental values: $IE_a(BF) = 11.12 \pm 0.01$ eV[35] from a photoelectron spectrum and $IE_a(BF) = 11.115 \pm 0.004$ eV obtained by extrapolating extensive Rydberg series.[36] Overall, the calculated results for BF are very good. The spectroscopic data and the ab initio calculations agree

TABLE 2: Spectroscopic Constants of BCl Derived from the REMPI Spectra[a]

isotopomer	upper electronic state	ν_{00}[b] (cm^{-1})	$\Delta G_{1/2}$ (cm^{-1})	ΔB_o (cm^{-1})	B_0'[c] (cm^{-1})	r_o (Å)	no. rot lines
$^{10}B^{35}Cl$	F $^1\Sigma^+$ (3sσ)	55 977.1 ± 1.8	1185 ± 3	0.1196 ± 0.001	0.8412 ± 0.003	1.6045 ± 0.004	40
$^{10}B^{37}Cl$	F $^1\Sigma^+$ (3sσ)	55 995 ± 10	1180 ± 3				
$^{11}B^{35}Cl$	F $^1\Sigma^+$ (3sσ)	55 971.8 ± 0.7	1129 ± 3	0.11120 ± 0.0005	0.7821 ± 0.002	1.6045 ± 0.006	43
$^{11}B^{37}Cl$	F $^1\Sigma^+$ (3sσ)	55 970.8 ± 1.6	1133 ± 3	0.1098 ± 0.001	0.7720 ± 0.003	1.6044 ± 0.006	44
$^{10}B^{35}Cl$	b $^3\Pi$ (3pπ)	56 870 ± 10					
$^{10}B^{37}Cl$	b $^3\Pi$ (3pπ)	56 862 ± 10					
$^{11}B^{35}Cl$	b $^3\Pi$ (3pπ)	56 864 ± 10					
$^{11}B^{37}Cl$	b $^3\Pi$ (3pπ)	56 863 ± 10					

[a] Uncertainties indicate the confidence of two standard deviations. [b] Listed uncertainty is the relative uncertainty (2σ) among the isotopomers. Absolute uncertainty (2σ) of all ν_{00} is 10 cm^{-1}. [c] B_0' for $^{11}B^{35}Cl$ is derived using $B_0'' = 0.67088 \pm 0.00009$ cm^{-1} from ref 19. The other isotopic species were derived using B_0'' obtained from reduced mass relationships; specifically, $B_0'' = 0.72165 \pm 0.00009$ cm^{-1} for $^{10}B^{35}Cl$ and $B_0'' = 0.66220 \pm 0.00009$ cm^{-1} for $^{11}B^{37}Cl$.

TABLE 3: Spectroscopic Constants of the States of $^{11}B^{19}F$

state	r_e (Å)	ν_{00} (cm^{-1})	T_e (cm^{-1})	ω_e (cm^{-1})	$\omega_e x_e$ (cm^{-1})	comment
		BF				
X $^1\Sigma^+$	1.263	0	0	1402	11.8	ref 42
calcd	1.265	0	0	1428	10.9	
a $^3\Pi$ (valence)	1.308	29 106	29 144	1324	9.2	ref 43
calcd	1.311	28 900	28 900	1343	9.5	
A $^1\Pi$ (valence)	1.304	51 089	51 158	1265	12.5	refs 36, 44
calcd	1.306	51 700	51 800	1289	13.7	
b $^3\Sigma^+$ (3sσ)	1.215	61 146	61 035	1629	22.3	refs 45, 46
calcd	1.216	61 600	61 500	1676	22.7	
B $^1\Sigma^+$ (3sσ)	1.207	65 499	65 354	1694	12.6	refs 44, 36
calcd	1.209	66 200	66 000	1733	13.0	
c $^3\Sigma^+$ (3pσ)	(1.228)	67 118	67 045	(1541)		ref 45
calcd	1.224	67 300	67 200	1595	13.5	
C $^1\Sigma^+$ (3pσ)	1.220	69 135	69 030	1613	14.5	refs 44, 36
calcd	1.220	69 400	69 300	1654	15.7	
d $^3\Pi$ (3pπ)	1.210		70 710	1697	11.0	ref 36
calcd	(no calc)					
D $^1\Pi$ (3pπ)	1.219	72 286	72 144	(1662)	11.7	ref 44
calcd	1.220	72 700	72 600	1719	11.8	
$^3\Delta$ (3dδ)						(no data)
calcd	1.211	77 400	77 200	1742	16.2	predissociated
E $^1\Delta$ (3dδ)	(1.222)	76 384	(76 292)	(1581)		refs 47, 36
calcd	1.213	77 300	77 100	1715	17.1	predissociated
G $^1\Sigma^+$ (4sσ)		77 096	76 952			refs 47, 36
calcd		{78 900}[a]				
F $^1\Pi$ (3dπ)		77 543	77 406(est)			ref 36
calcd		{77 700}[a]				
H $^1\Sigma^+$ (3dσ)		78 691	79 389			ref 36
calcd		{77 400}[a]				
I $^1\Sigma^+$ (4pσ)		79 763	79 631			ref 36
calcd		(79 900)[a]				
		BF^+				
X $^2\Sigma^+$	1.208 ± 0.005[b]	$IE_a(BF) = 11.115 \pm 0.004$ eV[c]		1765 ± 20[b]		
calcd	1.211	$IE_a(BF) = 11.10 \pm 0.02$ eV		1737	11.4	

[a] This estimate was computed using single-point calculations at internuclear distances of $r = 1.265$ Å for the ground state and $r = 1.211$ Å for the excited state. See text. [b] Ref 35. [c] Ref 36.

throughout the electronic manifold and accurately predict the energies of the $n = 3$ and $n = 4$ Rydberg states.

The results for BCl and BCl^+ are presented in Table 4, along with available experimental data. The limited comparison (for the X, a, and A states) suggests that the results for BCl are as reliable as those for BF. The computed adiabatic ionization energy of BCl is $IE_a(BCl) = 9.96 \pm 0.04$ eV. This is in agreement with $IE_a(BCl) = 10.03 \pm 0.1$ eV[9] obtained from an electron impact measurement and also with $IE_a(BCl) = 10.01 \pm 0.08$ eV[9] obtained from a reanalysis of dissociative photoionization data.[37]

Discussion

The present experimental data and ab initio results lead to consistent state assignments of the known spectra of BCl. As indicated in Tables 3 and 4, most upper electronic states of BF and BCl have predominately Rydberg character. Such Rydberg states align into Rydberg series characterized by quantum defects similar to those of atomic boron, which are $\delta(ns) \approx 0.7-1.0$, $\delta(np) \approx 0.54$, $\delta(nd) \approx 0.0-0.04$.[38,39] The F $^1\Sigma^+$ state of BCl is assigned as the 3sσ Rydberg state based upon the agreement between the predicted and the observed ν_{00}, ω_e, and state symmetry (Table 4). We use the ab initio value $IE_a(BCl) = 9.96$ eV and the experimental value $IE_a(BF) = 11.115$ eV for computing quantum defects δ of Rydberg states. Thus, the quantum defect of the F $^1\Sigma^+$ (3sσ) state of BCl is a satisfactory $\delta = 0.88$, nearly the same as the $\delta = 0.87$ that characterizes the B $^1\Sigma^+$ (3sσ) state of BF.[36] By absorbing one laser photon, the F $^1\Sigma^+$ (3sσ) state may form BCl^+ (X $^2\Sigma^+$); therefore, the ion signal forms through a 2 + 1 REMPI mechanism.

TABLE 4: Spectroscopic Constants of the States of $^{11}B^{35}Cl$

state	r_e (Å)	ν_{00} (cm^{-1})	T_e (cm^{-1})	ω_e (cm^{-1})	$\omega_e x_e$ (cm^{-1})	comment
			BCl			
X $^1\Sigma^+$	1.716	0	0	839	5.1	refs 48, 49, 19, 50, 18
calcd	1.713	0	0	864	5.6	
a $^3\Pi_1$	1.698	20 236	20 200	911	5.7	ref 19
calcd	1.699	19 900	19 800	926	5.8	
A $^1\Pi$	1.689	36 754	36 751	849	11.4	refs 49, 51, 52
calcd	1.692	37 200	37 200	868	11.5	
f $^3\Sigma^+$ (3sσ)	(no data)					
calcd	1.590	54 100	53 900	{1091}[a]		predissociated
F $^1\Sigma^+$ (3sσ)	(1.605)[b]	55 972		1129		this work
calcd	1.591	56 700	56 500	1179	11.9	predissociated
b $^3\Sigma^+$ (3pσ)		(56 854)[c]				this work
calcd	1.651	59 200	59 200			one quasi-bound level; see text
B $^1\Sigma^+$ (3pσ)	(1.636)[b]	60 429		870		ref 12
calcd	1.620	61 000	61 000	{904}[a]		predissociated
c $^3\Pi$ (3pπ)						
calcd	1.582	61 600	61 500	1191	7.2	predissociated
C $^1\Pi$ (3pπ)	(1.604)[b]	61 486		1170	7.3	ref 12
calcd	1.581	61 900	61 700	1194	7.0	predissociated
D $^1\Sigma^+$ (3dσ)	(1.61)[b]	65 866		1042		ref 12
calcd			{66 300}[d]			
E	(1.79)[b]	66 174				designated as E $^1\Sigma^+$ in ref 12; see text
calcd						
$^1\Delta$ (3dδ)						
calcd			{66 900}[d]			
$^1\Delta$ (mixed)[e]						
calcd			{68 800}[d]			
$^1\Pi$ (3dπ)						
calcd			{69 000}[d]			
$^1\Sigma^+$ (4sσ)						
calcd			{69 900}[d]			
$^1\Sigma^+$ (4pσ)						
calcd			{71 000}[d]			
$^1\Pi$ (4pπ)						
calcd			{71 300}[d]			
			BCl^+			
X $^2\Sigma^+$		$IE_a(BCl) = 10.0 \pm 0.1$ eV				ref 9; see text
calcd	1.594	$IE_a(BCl) = 9.96 \pm 0.04$ eV		1174	7.2	

[a] $\Delta G_{1/2}$ interval. [b] Value of r_0 instead of r_e. [c] Tentative assignment. See text. [d] This estimate was computed using single-point calculations at internuclear distances of $r = 1.713$ Å for the ground state and $r = 1.594$ Å for the excited state. See text. [e] Mixture of Rydberg and valence character.

TABLE 5: Basis Set Extrapolations (aug-cc-pV*n*Z) for the HF, CCSD, and (T) Contributions to the Ionization Energies of BF and BCl[a]

n	HF	CCSD	(T)	total
		$IE_a(BF)$		
3	9.825	1.206	0.037	11.067
4	9.806	1.239	0.041	11.087
5	9.803	1.243	0.043	11.089
extrap 3 to 4	9.806	1.264	0.044	11.114
extrap 4 to 5	9.803	1.248	0.045	**11.095**
		$IE_a(BCl)$		
3	8.760	1.114	0.033	9.907
4	8.746	1.172	0.039	9.957
5	8.742	1.175	0.041	9.958
extrap 3 to 4	8.746	1.214	0.043	10.004
extrap 4 to 5	8.742	1.178	0.044	**9.964**

[a] Zero-point vibrational energy is included. Best values are in boldface. Quantities are in eV.

In a previous study of ultraviolet absorption spectra, Verma[12] reported spectroscopic constants, symmetry assignments, and Rydberg orbital assignments for the B $^1\Sigma^+$, C $^1\Pi$, and D $^1\Sigma^+$ states of BCl. Although the rotational assignments established the state symmetries, the Rydberg orbital assignments were made under the presumption that the B $^1\Sigma^+$ state is the lowest energy (3sσ) Rydberg state. This initial assignment aligned the D $^1\Sigma^+$ state as the next series member and lowered the predicted IE_a(BCl). Since this study has found the lower energy F $^1\Sigma^+$ (3sσ) state, the previous Rydberg assignments are in error. In Table 4, we present revised B, C, and D state assignments that are supported by the accord among the observed and the predicted r_0, ν_{00}, and ω_e. The new assignments are also consistent with the present IE_a(BCl) and give the reasonable quantum defects $\delta(3p\sigma) \approx 0.65$, $\delta(3p\pi) \approx 0.59$, and $\delta(3d\sigma) \approx 0.25$, respectively. Presumably, the large $\delta(3d\sigma)$ quantum defect reflects the interaction of the boron 3dσ Rydberg orbital with the chlorine atom.

The b−X system is characterized by a solitary origin band at $\lambda_{laser} = 351.6$ nm. The ab initio results, summarized in Table 4, predict the $^3\Sigma^+$ (3pσ) state to reside near 52 900 cm^{-1} and to appear near 340 nm through a 2 + 1 REMPI mechanism. The calculations also indicate that the $^3\Sigma^+$ (3pσ) state supports only one quasi-bound vibrational level, accounting for the sparse nature of the spectrum. Since the calculations predict no unaccounted states near 28 500 cm^{-1}, we rule out assigning the b−X band to an electronic state residing at the energy of one laser photon. The quantum defect of the b $^3\Sigma^+$ (3pσ) state is $\delta = 0.84$, which is similar to the quantum defect, $\delta = 0.79$, derived for the corresponding c $^3\Sigma^+$ (3pσ) state of BF. We note that the isovalent AlF and AlCl molecules also exhibit REMPI spectra assigned to singlet−triplet transitions.[40,41]

Ultraviolet absorption spectroscopy has also characterized the E state ($\nu_{00} = 66\,174$ cm^{-1}), the highest energy electronic state

known for BCl.[12] A rotational analysis of the origin band supports a $^1\Sigma^+$ symmetry assignment, suggesting a Rydberg assignment of 4sσ. However, this assignment would imply an unreasonably large quantum defect, $\delta = 1.22$. The ab initio calculations predict the $^1\Sigma^+$ (4sσ) state to lie at higher energy near 69 900 cm^{-1} (Table 4) and to manifest $\delta \approx 0.76$, which is consistent with the defect observed for the F $^1\Sigma^+$ (3sσ) state. The calculations suggest no alternative assignments of $^1\Sigma^+$ symmetry. We note that $^3\Delta$ and $^3\Pi$ states reside in this energy range (Table 4); however, transitions to these states should exhibit more rotational structure than was reported.[12]

References and Notes

(1) Flamm, D. *Solid State Technol.* **1993**, *36*, 49.
(2) Pearton, S. J.; Hobson, W. S.; Abernathy, C. R.; Ren, F.; Fullowan, T. R.; Katz, A.; Perley, A. P. *Plasma Chem. Plasma Process.* **1993**, *13*, 311.
(3) Burton, R. H.; Gottscho, R. A.; Smolinsky, G. *Dry Etching for Microelectronics*; Elsevier: New York, 1984.
(4) Sonek, G. J.; Ballantyne, J. M. *J. Vac. Sci. Technol., B* **1984**, *2*, 653.
(5) Scheller, G. R.; Gottscho, R. A.; Intrator, T.; Graves, D. B. *J. Appl. Phys.* **1988**, *64*, 4384.
(6) Jabbour, Z. J.; Martus, K. E.; Becker, K. *Bull. Am. Phys. Soc.* **1988**, *33*, 941.
(7) Gilbert, P. G.; Siegel, R. B.; Becker, K. *Phys. Rev. A* **1990**, *41*, 5594.
(8) Chase, M. W., Jr. *J. Phys. Chem. Ref. Data, Monogr.* **1998**, *9*, 1.
(9) Hildenbrand, D. *J. Chem. Phys.* **1996**, 10507.
(10) Lias, S. G.; Bartmess, J. E.; Liebman, J. F.; Holmes, J. L.; Levin, R. D.; Mallard, W. G. *J. Phys. Chem. Ref. Data, Suppl.* **1988**, *17* (1), 1.
(11) Srivastava, R. D.; Farber, M. *J. Chem. Soc., Faraday Trans.* **1971**, *67*, 2298.
(12) Verma, R. D. *J. Mol. Spectrosc.* **1995**, *169*, 295.
(13) Baeck, K. K.; Bartlett, R. J. *J. Chem. Phys.* **1997**, *106*, 4604.
(14) Bauschlicher, C. W., Jr.; Ricca, A. *J. Phys. Chem. A* **1999**, *103*, 4313.
(15) Johnson, R. D., III; Tsai, B. P.; Hudgens, J. W. *J. Chem. Phys.* **1988**, *89*, 4558.
(16) Daly, N. R. *Rev. Sci. Instrum.* **1960**, *31*, 264.
(17) Herzberg, G. *Spectra of Diatomic Molecules*, 2nd ed.; Molecular Spectra and Molecular Structure Series; Van Nostrand Reinhold: New York, 1950; Vol. 1.
(18) Maki, A. G.; Lovas, F. J.; Suenram, R. D. *J. Mol. Spectrosc.* **1982**, *91*, 424.
(19) Lebreton, J.; Marsigny, L.; Ferran, J. *C. R. Acad. Sci. Paris, Ser. C* **1971**, *272*, 1094.
(20) Stanton, J. F.; Bartlett, R. J. *J. Chem. Phys.* **1993**, *98*, 7029.
(21) Dunning, T. H., Jr. *J. Chem. Phys.* **1989**, *90*, 1007.
(22) Woon, D. E.; Dunning, T. H., Jr. *J. Chem. Phys.* **1993**, *98*, 1358.
(23) Bauschlicher, C. W., Jr.; Ricca, A. *J. Phys. Chem. A* **1998**, *102*, 4722.
(24) Martin, J. M. L.; Uzan, O. *Chem. Phys. Lett.* **1998**, *282*, 16.
(25) Bauschlicher, C. W., Jr.; Ricca, A. *J. Phys. Chem. A* **1998**, *102*, 8044.
(26) Marston, C. C.; Balint-Kurti, G. G. *J. Chem. Phys.* **1989**, *91*, 3571.
(27) Raghavachari, K.; Trucks, G. W.; Pople, J. A.; Head-Gordon, M. *Chem. Phys. Lett.* **1989**, *157*, 479.
(28) Bauschlicher, C. W., Jr.; Martin, J. M. L.; Taylor, P. R. *J. Phys. Chem. A* **1999**, *103*, 7715.
(29) Helgaker, T.; Klopper, W.; Koch, H.; Noga, J. *J. Chem. Phys.* **1997**, *106*, 9639.
(30) Lias, S. G. In *NIST Chemistry WebBook*; Mallard, W. G., Linstrom, P. J., Eds.; NIST Standard Reference Database No. 69; National Institute of Standards and Technology: Gaithersburg, MD, 1998. http://webbook.nist.gov/chemistry/.
(31) Bartmess, J. E. In *NIST Chemistry WebBook*; Mallard, W. G., Linstrom, P. J., Eds.; NIST Standard Reference Database No. 69; National Institute of Standards and Technology: Gaithersburg, MD, 1998. http://webbook.nist.gov/chemistry/.
(32) Stanton, J. F.; Gauss, J.; Watts, J. D.; Lauderdale, W. J.; Bartlett, R. J. *Int. J. Quantum Chem.* **1992**, *S26*, 879.
(33) Stanton, J. F.; Gauss, J.; Watts, J. D.; Nooijen, M.; Oliphant, N.; Perera, S. A.; Szalay, P. G.; Lauderdale, W. J.; Kucharski, S. A.; Gwaltney, S. R.; Beck, S.; Balková, A.; Bernholdt, D. E.; Baeck, K.-K.; Rozyczko, P.; Sekino, H.; Hober, C.; Bartlett. R. J. *ACES II*, release 3.0; Integral packages included are VMOL (Almlöf, J.; Taylor, P. R.); VPROPS (Taylor, P.); ABACUS (Helgaker, T.; Jensen, H. J. Aa.; Jørgensen, P.; Olsen, J.; Taylor, P. R.); Program product of the Quantum Theory Project, University of Florida.
(34) Certain commercial materials and equipment are identified in this paper to specify procedures completely. In no case does such identification imply recommendation or endorsement by the National Institute of Standards and Technology, nor does it imply that the material or equipment identified is necessarily the best available for the purpose.
(35) Dyke, J. M.; Kirby, C.; Morris, A. *J. Chem. Soc., Faraday Trans. 2* **1983**, *79*, 483.
(36) Caton, R. B.; Douglas, A. E. *Can. J. Phys.* **1970**, *48*, 432.
(37) Dibeler, V. H.; Walker, J. A. *Inorg. Chem.* **1969**, *8*, 50.
(38) Martin, W. C.; Sugar, J.; Musgrove, A. *NIST Atomic Spectra Database*, version 2.0; National Institute of Standards and Technology: Gaithersburg, MD, 1999. http://physics.nist.gov/cgi-bin/AtData/main_asd.
(39) Irikura, K. K.; Johnson, R. D., III; Hudgens, J. W. *J. Opt. Soc. Am. B* **1993**, *10*, 763.
(40) Dearden, D. V.; Johnson, R. D., III; Hudgens, J. W. *J. Chem. Phys.* **1993**, *99*, 7521.
(41) Dearden, D. V.; Johnson, R. D., III; Hudgens, J. W. *J. Phys. Chem.* **1991**, *95*, 4291.
(42) Lovas, F. J.; Johnson, D. R. *J. Chem. Phys.* **1971**, *55*, 41.
(43) Lebreton, J.; Ferran, J.; Marsigny, L. *J. Phys. B* **1975**, *8*, 465.
(44) Chretien, M.; Miescher, E. *Nature (London)* **1949**, *163*, 996.
(45) Strong, H. M.; Knauss, H. P. *Phys. Rev.* **1936**, *49*, 740.
(46) Paul, F. W.; Knauss, H. P. *Phys. Rev.* **1938**, *54*, 1072.
(47) Robinson, D. W. *J. Mol. Spectrosc.* **1963**, *11*, 275.
(48) Endo, Y.; Shuji, S.; Hirota, E. *Bull. Chem. Soc. Jpn.* **1983**, *56*, 3410.
(49) Herzberg, G. R.; Hushley, W. *Can. J. Res. Sect. A* **1941**, *19*, 127.
(50) Miescher, E. *Helv. Phys. Acta* **1935**, *8*, 279.
(51) Verma, R. D. *J. Mol. Spectrosc.* **1961**, *7*, 145.
(52) Verma, R. D. *Can. J. Phys.* **1962**, *40*, 1852.